

Deep Reinforcement Learning Based Optimal Infinite-Horizon Control of Probabilistic Boolean Control Networks

Jingjie Ni, Fangfei Li, *Member, IEEE*, Zheng-Guang Wu, *Member, IEEE*

Abstract—In this paper, a deep reinforcement learning based method is proposed to obtain optimal policies for optimal infinite-horizon control of probabilistic Boolean control networks (PBCNs). Compared with the existing literatures, the proposed method is model-free, namely, the system model and the initial states needn't to be known. Meanwhile, it is suitable for large-scale PBCNs. First, we establish the connection between deep reinforcement learning and optimal infinite-horizon control, and structure the problem into the framework of the Markov decision process. Then, PBCNs are defined as large-scale or small-scale, depending on whether the memory of the action-values exceeds the RAM of the computer. Based on the newly introduced definition, Q-learning (QL) and double deep Q-network (DDQN) are applied to the optimal infinite-horizon control of small-scale and large-scale PBCNs, respectively. Meanwhile, the optimal state feedback controllers are designed. Finally, two examples are presented, which are a small-scale PBCN with 3 nodes, and a large-scale one with 28 nodes. To verify the convergence of QL and DDQN, the optimal control policy and the optimal action-values, which are obtained from both the algorithms, are compared with the ones based on a model-based method named policy iteration. Meanwhile, the performance of QL is compared with DDQN in the small-scale PBCN.

Index Terms—Deep reinforcement learning, model-free, probabilistic Boolean control networks, infinite-horizon optimal control

I. INTRODUCTION

THE control of gene regulatory networks is a key problem in systems biology. In 1969, Kauffman [1] proposed Boolean networks (BNs) to model the dynamics of gene regulatory networks. In BNs, a Boolean variable “0” or “1” is used to represent whether a gene is transcribed or not. To describe the more complex behavior of gene regulatory

networks, probabilistic Boolean networks (PBNs) have been proposed [2]. PBNs are more general BNs that can describe random switching during gene regulation. Many gene regulatory networks have exogenous inputs, so PBNs are naturally extended to probabilistic Boolean control networks (PBCNs). Fundamental control problems of PBCNs have been carried out, such as controllability [3], [4], stabilization [5]–[7], finite-time stabilization [8]–[10], observability [11], [12], output tracking [13], and finite-time output tracking [14]. Among them, optimal control of PBCNs is still an important problem, which is worth further study.

The objective of optimal control for a PBCN is to find optimal control policies, which minimize the cost-to-go function related to a control goal. Relevant research can be applied to therapeutic intervention [15], [16]. For instance, the optimal policy obtained in [15] is successfully utilized in the melanoma gene-expression network to reduce the occurrence of undesired states. The other application of the study is engine control [17],

Optimal control of PBCNs can be divided into finite-horizon and infinite-horizon. The problems with finite-horizon have been considered in [18]–[20]. Optimal infinite-horizon control of PBCNs is required for persistence problems. Unlike the one with finite-horizon, optimal infinite-horizon control of PBCNs does not necessarily have a limited cost-to-go function. The discounted factor has been introduced to guarantee the existence of solutions. Compared with optimal finite-horizon control, the design of the optimal infinite-horizon controller is more challenging due to increased computational complexity.

To solve optimal infinite-horizon control of PBCNs, policy iteration [21]–[25], QL [15], and sampling-based path integral [16] have been presented. Although the above methods are highly efficient, they have some limitations. Policy iteration is a matrix-based method with the assumption that the system models of PBCNs are known. However, it cannot deal with large-scale PBCNs since the operation of gigantic metrics is infeasible. Meanwhile, the perfectly accurate systems models of PBCNs are impossible, and PBCNs with complex construction is difficult to be modeled due to computational complexity. To deal with modeling difficulty, model-free sampling-based path integral [16] and QL [15] are considered. Nevertheless, QL [15] is not applicable to large-scale systems, and sampling-based path integral [16] only provides an optimal policy according to a given initial state.

To overcome the limitations mentioned above, DDQN, a deep reinforcement method, is considered. The connection

This work was supported by the National Natural Science Foundation of China under Grants 62233005, 62173142, and the Programme of Introducing Talents of Discipline to Universities (the 111 Project) under Grant B17017.

Jingjie Ni is with the School of Mathematics, East China University of Science and Technology, Shanghai, 200237, P.R. China (email: njingjie20000504@163.com).

Fangfei Li is with the School of Mathematics, East China University of Science and Technology, Shanghai, 200237, P.R. China. Meanwhile, she is also with the Key Laboratory of Smart Manufacturing in Energy Chemical Process, Ministry of Education, East China University of Science and Technology, Shanghai, 200237, P.R. China (email: li.fangfei@163.com; lifangfei@ecust.edu.cn).

Zheng-Guang Wu is with the Institute of Cyber-Systems & Control, Zhejiang University, Hangzhou, Zhejiang, 310027, P.R. China (email: nashwzhg@zju.edu.cn).

between reinforcement learning and optimal infinite-horizon control is revealed in [26]. A simple version of DDQN is QL [27], which is a model-free algorithm in reinforcement learning with convergence guarantee [28]. Using QL, an agent under the framework of the Markov decision process can learn optimal control policies through interaction with the environment [26], [29]. For PBCNs without known models, QL presents a more direct way to obtain optimal policy since the modeling step is skipped. QL has been widely used in control problems of gene regulatory networks, such as feedback stabilization of PBCNs [30], [31], and optimal infinite-horizon control of PBCNs under state-flipped control [15]. For a gene regulatory network containing too many nodes, QL is no longer valid due to *curse of dimensionality*, and deep Q-network [32] in deep reinforcement learning needs to be considered. Deep Q-network is the combination of QL and deep learning. The advantage of deep Q-network over QL is its ability to solve problems with large state space. DDQN is an advanced version of deep Q-network [33], which decreases the overestimation in action-values of deep Q-network. DDQN only needs to add a network on the basis of deep Q-network, which is relatively simple compared with other methods to improve the performance of deep Q-network. Therefore, DDQN has been applied in various studies, such as controllability of PBCNs under external perturbations [34], and output tracking of PBCNs [35]. Although many control problems of PBCNs based on QL and DDQN have been investigated, most of them focus on controllability and stabilization [30], [31], [34], [35]. It is worth noting that the optimal infinite-horizon control of PBCN based on deep reinforcement learning is still an open problem.

Taken together, in this paper we utilize model-free QL and DDQN to obtain optimal control policies for small-scale and large-scale PBCNs. The main contributions of our paper are listed as follows.

- 1) In Theorem 1, we prove that reinforcement learning provides an optimization framework to solve the infinite horizon problem, which can be easily framed as a minimization problem.
- 2) QL and DDQN for optimal infinite-horizon control of PBCNs are proposed. Unlike [21]–[25] and [16], our method does not need the knowledge of system models or initial states.
- 3) Optimal infinite-horizon control of large-scale PBCNs is solved in this paper, which cannot be solved by using model-based methods proposed in [21]–[25], as well as QL in [15].

The framework of this paper is organized as follows. In Section II, we introduce the basic concepts of the Markov decision process, QL, and DDQN. In Section III, we give the system models of PBCN. Then, we structure optimal infinite-horizon control of PBCNs into the framework of the Markov decision process, and reveal the relationship between deep reinforcement learning and optimal control. Next, we propose optimal infinite-horizon control of small-scale and large-scale PBCNs using QL and DDQN, respectively. In Section IV, a small-scale PBCN with 3 nodes and a large-scale one with 28

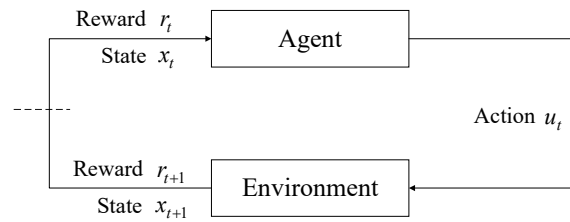


Fig. 1: Markov decision process

nodes are considered to verify the proposed method. Finally, the conclusions are given in Section V.

Notations: \mathbb{Z}^+ , \mathbb{R}^+ , \mathbb{R} denotes the sets of nonnegative integers, nonnegative real numbers, and real numbers, respectively. $\mathbb{E}[\cdot]$ is the expected value operator. $\text{var}[\cdot]$ is the variance. $\Pr\{A | B\}$ is the probability of the event A under the condition of the event B . For a set D , $|D|$ is the number of elements. There are three basic operations on Boolean variables, which are “not”, “and” and “or”, expressed as \neg , \wedge , and \vee , respectively. $\mathcal{B} := \{0, 1\}$ is the Boolean domain, and $\mathcal{B}^n := \underbrace{\mathcal{B} \times \dots \times \mathcal{B}}_n$.

II. PRELIMINARIES

In this section, we introduce deep reinforcement learning, which lays the foundation for solving optimal infinite-horizon control of PBCNs. First, we introduce the framework of reinforcement learning, namely the Markov decision process. Then, we introduce two algorithms named QL and DDQN.

A. Markov Decision Process

The schematic diagram of the Markov decision process is shown in Figure 1. Let a quintuple $(\mathbf{X}, \mathbf{U}, \gamma, \mathbf{P}, \mathbf{R})$ represent the Markov decision process, where $\mathbf{X} = \{x_t, t \in \mathbb{Z}^+\}$ is the state space, $\mathbf{U} = \{u_t, t \in \mathbb{Z}^+\}$ is the action space, $0 \leq \gamma < 1$ is the discount factor, $\mathbf{P}_{x_t}^{x_{t+1}}(u_t) = \Pr\{x_{t+1} | x_t, u_t\}$ is the state-transition probability from state x_t to x_{t+1} when action u_t is taken, and $\mathbf{R}_{x_t}^{x_{t+1}}(u_t) = \mathbb{E}[r_{t+1} | x_t, u_t]$ with $r_{t+1} = r_{t+1}(x_t, u_t)$ is the expected reward. The Markov decision process is the framework for an agent to find an optimal policy through interaction with the environment. At each time step $t \in \mathbb{Z}^+$, the agent observes a state x_t and selects an action u_t , according to the policy $\pi : x_t \rightarrow u_t, \forall t \in \mathbb{Z}^+$. Then, the environment gives a reward r_{t+1} and a new state x_{t+1} . The agent obtains r_{t+1} which reveals the advantage to take u_t at x_t , and then updates π .

Define $G_t = \sum_{i=t+1}^{\infty} \gamma^{i-t-1} r_i$ as the return. The goal of the agent is to find the optimal deterministic policy $\pi^* : x_t \rightarrow u_t, \forall t \in \mathbb{Z}^+$, under which the expected return $\mathbb{E}_{\pi}[G_t], \forall t \in \mathbb{Z}^+$ is maximized. $q_{\pi}(x_t, u_t)$ is the value of taking the action u_t at the state x_t and thereby following the policy π , which is a detailed version of $\mathbb{E}_{\pi}[G_t]$:

$$q_{\pi}(x_t, u_t) = \mathbb{E}_{\pi}[G_t | x_t, u_t], \quad (1)$$

and satisfies the Bellman equation:

$$q_{\pi}(x_t, u_t) = \sum_{x_{t+1} \in \mathbf{X}} \mathbf{P}_{x_t}^{x_{t+1}}(u_t) [\mathbf{R}_{x_t}^{x_{t+1}}(u_t) + \gamma q_{\pi}(x_{t+1}, \pi(x_{t+1}))]. \quad (2)$$

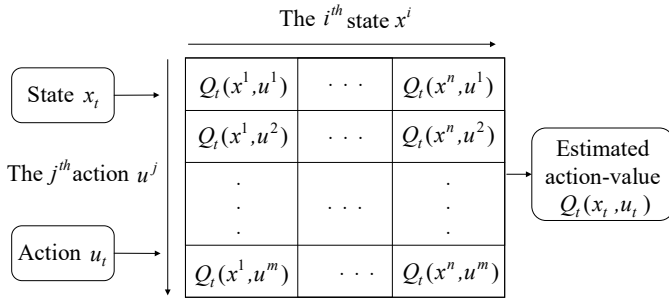


Fig. 2: Q-table

Equation (2) reveals the recursion of $q_\pi(x_t, u_t)$, which is critical for the algorithms introduced in the following subsection.

The optimal action-value is defined as follows:

$$q^*(x_t, u_t) = \max_{\pi \in \Pi} q_\pi(x_t, u_t), \forall x_t \in \mathbf{X}, \forall u_t \in \mathbf{U}, \quad (3)$$

where Π is the set of all admissible policies. Based on $q^*(x_t, u_t)$, π^* can be obtained as follows:

$$\pi^*(x_t) = \arg \max_{u_t \in \mathbf{U}} q^*(x_t, u_t), \forall x_t \in \mathbf{X}. \quad (4)$$

For problems under the framework of the Markov decision process, π^* can be obtained through many algorithms, e.g., policy iteration. However, the premise of these algorithms is stringent to optimal infinite-horizon control of PBCNs. In particular, the model including \mathbf{P} should be known, whereas modeling PBCNs is difficult. Therefore, we introduce a model-free technique, namely QL .

B. Q-Learning

QL is a classical algorithm in reinforcement learning. For a problem in the framework of the Markov decision process with an unknown model, an agent can obtain π^* through interaction with the environment using QL .

As shown in Figure 2, the Q -table is used to record each $Q_t(x_t, u_t)$, which is the estimate of $q^*(x_t, u_t)$. At each time step t , the Q -table updates once, using the rule given as follows:

$$Q_{t+1}(x, u) = \begin{cases} (1 - \alpha_t)Q_t(x, u) + \alpha_t TDE_t, & \text{if } (x, u) = (x_t, u_t), \\ Q_t(x, u), & \text{else,} \end{cases} \quad (5)$$

where $\alpha_t \in (0, 1]$, $t \in \mathbb{Z}^+$ is the learning rate, and TDE_t is the temporal-difference (TD) error:

$$TDE_t = r_{t+1} + \gamma \max_{u_{t+1} \in \mathbf{U}} Q_t(x_{t+1}, u_{t+1}) - Q_t(x_t, u_t). \quad (6)$$

ϵ -greedy method is used for an agent to select an action:

$$u_t = \begin{cases} \arg \max_{u_t \in \mathbf{U}} Q_t(x_t, u_t), & P = 1 - \epsilon, \\ \text{rand}(\mathbf{U}), & P = \epsilon, \end{cases} \quad (7)$$

where $\text{rand}(\mathbf{U})$ represents an action u_t which is randomly selected from the action space \mathbf{U} . Following the ϵ -greedy method, an agent not only tests new actions to find a better policy but also develops the current optimal policy.

Under certain conditions, $Q_t(x_t, u_t)$ converges to the fixed

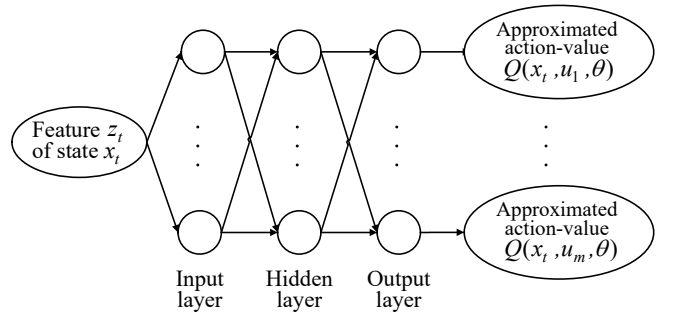


Fig. 3: Artificial neural network with one hidden layer

point $q^*(x_t, u_t)$ with probability one [28]:

$$\lim_{t \rightarrow \infty} Q_t(x_t, u_t) = q^*(x_t, u_t), \forall x_t \in \mathbf{X}, \forall u_t \in \mathbf{U}. \quad (8)$$

Substitute (8) into (4), the optimal policy π^* is obtained as follows:

$$\pi^*(x_t) = \arg \max_{u_t \in \mathbf{U}} \lim_{t \rightarrow \infty} Q_t(x_t, u_t), \forall x_t \in \mathbf{X}. \quad (9)$$

The limitation of QL is that it cannot solve problems with large state space. In particular, the operation of QL is based on a Q -table, which requires enough memory to store $|\mathbf{X}| \times |\mathbf{U}|$ values. When the state space \mathbf{X} is so large that the memory of $|\mathbf{X}| \times |\mathbf{U}|$ values exceeds the capabilities of modern computers, QL is no longer applicable. For these problems, we introduce $DDQN$.

C. Double Deep Q-Network

$DDQN$ is an algorithm in deep reinforcement learning, which is the combination of deep learning and QL . The difference between $DDQN$ and QL lies in the expression of estimated action-values. QL uses a Q -table to represent estimated action-values, while $DDQN$ uses function approximation. Due to the difference, $DDQN$ no longer needs a large memory to store $|\mathbf{X}| \times |\mathbf{U}|$ values. Thus, it is suitable for problems with large state space.

Artificial neural networks are used for function approximation. A good property of artificial neural networks is that they can fit any function. The structure of the artificial neural network with a hidden layer is shown in Figure 3. Given the feature z_t of the state x_t , the outputs of the artificial neural network are the approximated action-values of taking u_i , $i = 1, \dots, m$, at x_t :

$$Q(x_t, u_i, \theta) = F_l(w_l(\dots F_2(w_2 F_1(w_1 z_t + b_1) + b_2) \dots) + b_l), i = 1, \dots, m, \quad (10)$$

where l represents the number of layers. F_j , $w_j \in \mathbb{R}^{n_j} \times \mathbb{R}^{n_{j+1}}$, and $b_i \in \mathbb{R}^{n_j}$ represent the activation function, the weight matrix, and the bias vector of the j^{th} layer respectively. Besides, $\theta = \{w_j, b_j\}_{j=1}^l$ is the set of parameters.

The objective of the artificial neural network is to fit the optimal action-value function, and then obtain the optimal policy:

$$\begin{aligned} Q(x_t, u_t, \theta) &\approx q^*(x_t, u_t), \forall x_t \in \mathbf{X}, \\ \pi^*(x_t) &= \arg \max_{u_t \in \mathbf{U}} Q(x_t, u_t, \theta), \forall x_t \in \mathbf{X}. \end{aligned} \quad (11)$$

At each time step t , the artificial neural network updates θ to reduce the loss function $L(\theta)$, which is given as follows:

$$L(\theta) = \frac{1}{M} \sum_i^M (y_i - Q(x_i, u_i, \theta))^2. \quad (12)$$

In (12), mini-batch size M is the number of samples, and y_i represents the i^{th} target value:

$$y_i = r_i + \gamma Q(x'_i, \arg \max_{u \in \mathcal{U}} Q(x'_i, u, \theta), \varphi), \quad (13)$$

where x'_i is the subsequent state of x_i , and φ is the target network. Polyak averaging is used for updating φ , namely $\varphi = \tau\varphi + (1 - \tau)\theta$, where $0 \leq \tau \leq 1$ is the learning rate of φ .

The selection of $y_i, i = 1, \dots, M$ is based on experience replay, which is a process of random sampling from the replay memory. The replay memory $D_k = \{e_1, \dots, e_k\}$ stores k latest Markov decision process sequences, where k represents the capacity of D_k . The purpose of experience replay is to achieve stability by breaking the temporal dependency among samples.

The artificial neural network reduces the loss function $L(\theta)$ (12) by updating the parameters θ with gradient descent:

$$\theta = \theta - \beta \nabla_{\theta} L(\theta), \quad (14)$$

where $0 < \beta \leq 1$ is the learning rate, and $\nabla_{\theta} L(\theta)$ is the gradient of $L(\theta)$ to θ .

III. OPTIMAL CONTROL OF PBCNs USING DEEP REINFORCEMENT LEARNING

In this section, we discuss optimal infinite-horizon control of PBCNs using deep reinforcement learning. The advantage of deep reinforcement learning in the problem lies in its model-free characteristic, which solves the difficulty of modeling PBCNs. First, we present the system model of PBCNs. Then, we use a model-free approach based on deep reinforcement learning to solve the problem. Specifically, we establish the connection between action-value functions in deep reinforcement learning and cost-to-go functions in traditional optimal infinite-horizon control, and structure the problem into the framework of the Markov decision process. Then, we propose optimal infinite-horizon control of PBCNs using *QL* and *DDQN*. The details of the proposed algorithms, such as the setting of parameters and the structure of artificial neural networks, are explained. Finally, we discuss the computational complexity of *QL* and *DDQN*, and then present the applicability of these two algorithms.

A. System Models for PBCNs

A PBCN with n nodes and m control inputs is defined as follows:

$$\begin{cases} x_1(t+1) = f_1^{(j)}(x_1(t), \dots, x_n(t), u_1(t), \dots, u_m(t)), \\ x_2(t+1) = f_2^{(j)}(x_1(t), \dots, x_n(t), u_1(t), \dots, u_m(t)), \\ \vdots \\ x_n(t+1) = f_n^{(j)}(x_1(t), \dots, x_n(t), u_1(t), \dots, u_m(t)), \end{cases} \quad t \in \mathbb{Z}^+, \quad (15)$$

where $x_i(t) \in \mathcal{B}, i \in \{1, \dots, n\}$ represents the i^{th} node at the time step t , and $u_j(t) \in \mathcal{B}, j \in \{1, \dots, m\}$ represents the j^{th}

control input at the time step t . All nodes at the time step t are represented by $x(t) = (x_1(t), \dots, x_n(t)) \in \mathcal{B}^n$. Similarly, all control inputs at the time step t are represented by $u(t) = (u_1(t), \dots, u_m(t)) \in \mathcal{B}^m$. Taking $x(t) \times u(t)$ as independent variables, and $x_i(t+1)$ as dependent variable, the logical function is described as $f_i^{(j)} \in \mathcal{F}_i = \{f_i^1, f_i^2, \dots, f_i^{l_i}\} : \mathcal{B}^{n+m} \rightarrow \mathcal{B}, j \in \{1, \dots, l_i\}$. A logical function $f_i^{(j)}$ is randomly selected from the set of logical functions $\{f_i^1, f_i^2, \dots, f_i^{l_i}\}$ with the probability $\{P_i^1, P_i^2, \dots, P_i^{l_i}\}$, where $\sum_{j=1}^{l_i} P_i^j = 1$ and $P_i^j \geq 0$.

Remark 1 : PBCNs, which can describe the random switching behaviors, are more general versions of Boolean control networks. When $l_i = 1, i = 1, \dots, n$, PBCNs degenerate into Boolean control networks.

B. Optimal Infinite-horizon Control of PBCNs in Markov decision process

For optimal infinite-horizon control of PBCNs, we aim to find the optimal deterministic control policy $\tilde{\pi}^* : x(t) \rightarrow u(t), \forall x(t) \in \mathcal{B}^n$ which minimizes the cost-to-go function:

$$J_{\tilde{\pi}}(x(t)) = \lim_{N \rightarrow \infty} \mathbb{E}_{\tilde{\pi}} \left[\sum_{i=t}^N \gamma^{i-t} l_{i+1} | x(t) \right], \quad \forall x(t) \in \mathcal{B}^n, \quad (16)$$

where $l_{i+1} = l_{i+1}(x(i), u(i)) \in \mathbb{R}^+$ is the cost. The discount factor γ ensures the finiteness of $J_{\tilde{\pi}}(x(t))$ for infinite-horizon, which prevents ill-posed optimization problems.

Lemma 1 : Consider (16), if there exists a constant $M \in \mathbb{R}^+$ such that $0 \leq l_{i+1} \leq M, \forall i \in \mathbb{Z}^+$, then $J_{\tilde{\pi}}(x(t))$ is bounded.

Proof : Notice that there exists a constant $M \in \mathbb{R}^+$ such that $0 \leq l_{i+1} \leq M, \forall i \in \mathbb{Z}^+$, consequently, we have:

$$\begin{aligned} J_{\tilde{\pi}}(x(t)) &= \lim_{N \rightarrow \infty} \mathbb{E}_{\tilde{\pi}} \left[\sum_{i=t}^N \gamma^{i-t} l_{i+1} | x(t) \right] \\ &= \mathbb{E}_{\tilde{\pi}} \left[\sum_{i=t}^{\infty} \gamma^{i-t} l_{i+1} | x(t) \right] \\ &= \sum_{i=t}^{\infty} \gamma^{i-t} \mathbb{E}_{\tilde{\pi}} [l_{i+1} | x(t)] \\ &\leq \sum_{i=t}^{\infty} \gamma^{i-t} M \\ &= \frac{M}{1 - \gamma}, \end{aligned}$$

where the second equality and the third one hold according to Theorem 1.4.44 and Corollary 1.4.46 of [36], respectively. Thus, $J_{\tilde{\pi}}(x(t))$ is bounded. \blacksquare

The introduction of γ brings new meaning to $J_{\tilde{\pi}}(x(t))$. $J_{\tilde{\pi}}(x(t))$ gives higher weights to recent costs, and lower weights to future costs. This definition is consistent with most control goals of PBCNs. For instance, optimal infinite-horizon control of PBCNs can be applied to cancer therapy, where the initial condition of patients is more concerned with the consideration of life expectancy.

The premise for using deep reinforcement learning in optimal infinite-horizon control of PBCNs is structuring the problem into the framework of the Markov decision process.

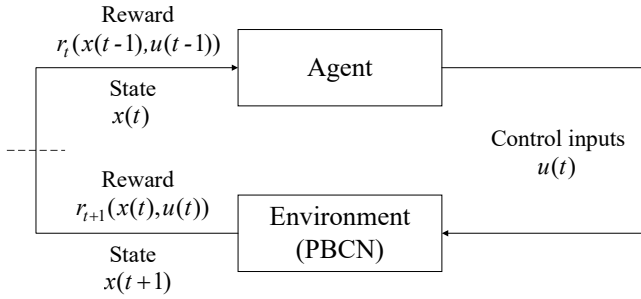


Fig. 4: Markov decision process for PBCNs

We represent the Markov decision process for optimal infinite-horizon control of PBCNs by the quintuple $(\mathcal{B}^n, \mathcal{B}^m, \gamma, \mathbf{P}, \mathbf{R})$. The details of the Markov decision process are shown in Figure 4. The environment is defined as the PBCN, and the agent is the machine that learns and provides the policy. The state space is represented by \mathcal{B}^n . A state is defined as $x_t = x(t)$. The action space is represented by \mathcal{B}^m . An action is defined as $u_t = u(t)$. The discount factor γ is valued in $[0, 1)$, according to the importance of the future reward. The state-transition probability \mathbf{P} is derived from the dynamics of PBCNs. The expected reward \mathbf{R} is the expectation of r_t .

It is assumed that the agent knows the state dimension n and the action dimension m , but does not know \mathbf{P} and \mathbf{R} . In other words, the agent only knows the number of nodes n and the number of control inputs m , but does not know the dynamics of the PBCN (15). Meanwhile, at each time step t , the agent is assumed to receive x_t and r_t given by the PBCN, and the PBCN is also assumed to receive u_t given by the agent. Each interaction between the agent and the environment helps the agent further understand \mathbf{P} and \mathbf{R} , which is reflected in a better estimation of $q^*(x_t, u_t)$ and a more in-depth knowledge of π^* .

Notice that the expression of the optimal policy in the Markov decision process is different from that in traditional optimal control. To be specific, π^* is defined as the one maximizes $q_\pi(x_t, u_t)$ in Markov decision process, whereas $\tilde{\pi}^*$ is defined as the one minimizes $J_{\tilde{\pi}}(x_t)$ in traditional optimal control. Next, we will show that π^* is equivalent to $\tilde{\pi}^*$ under certain reward settings.

Theorem 1 : Set $r_{i+1} = C_1 l_{i+1} + C_2, \forall i \in \mathbb{Z}^+$, where $C_1 < 0$ and C_2 are two constants, then π^* is equivalent to $\tilde{\pi}^*$.

Proof : First, we show that π^* minimizes $J_\pi(x_t), \forall x_t \in \mathbf{X}$. Since there exist two constants $C_1 < 0$ and C_2 such that $r_{i+1} = C_1 l_{i+1} + C_2, \forall i \in \mathbb{Z}^+$, it is easy to obtain $l_{i+1} = \frac{r_{i+1} - C_2}{C_1}, \forall i \in \mathbb{Z}^+$. Substitute $l_{i+1} = \frac{r_{i+1} - C_2}{C_1}$ into $J_\pi(x_t) = \lim_{N \rightarrow \infty} \mathbb{E}_\pi \left[\sum_{i=t}^N \gamma^{i-t} l_{i+1} | x_t \right]$, then we obtain

$$\begin{aligned} J_\pi(x_t) &= \mathbb{E}_\pi \left[\sum_{i=t}^{\infty} \gamma^{i-t} \frac{r_{i+1} - C_2}{C_1} | x_t \right] \\ &= \frac{1}{C_1} \mathbb{E}_\pi \left[\sum_{i=t}^{\infty} \gamma^{i-t} r_{i+1} | x_t \right] - \frac{C_2}{C_1} \sum_{i=t}^{\infty} \gamma^{i-t} \\ &= \frac{1}{C_1} \mathbb{E}_\pi \left[\sum_{i=t}^{\infty} \gamma^{i-t} r_{i+1} | x_t, \pi(x_t) \right] + \frac{C_2}{(1-\gamma)C_1} \\ &= \frac{1}{C_1} q_\pi(x_t, \pi(x_t)) + \frac{C_2}{(1-\gamma)C_1}. \end{aligned}$$

Recall that π^* maximizes $q_\pi(x_t, u_t), \forall x_t \in \mathbf{X}, \forall u_t \in \mathbf{U}$. Meanwhile, equation (4) indicates that $q_{\pi^*}(x_t, \pi^*(x_t)) = \max_{u_t} q^*(x_t, u_t)$. Thus, π^* maximizes $q_\pi(x_t, \pi(x_t)), \forall x_t \in \mathbf{X}$. Notice that only $\frac{1}{C_1} q_\pi(x_t, \pi(x_t))$ depends on π in the last equality, where $C_1 < 0$. Hence, we can conclude that π^* minimizes $J_\pi(x_t), \forall x_t \in \mathbf{X}$.

Next, we show that $\tilde{\pi}^*$ maximizes $q_\pi(x_t, u_t), \forall x_t \in \mathbf{X}, \forall u_t \in \mathbf{U}$. Substitute $r_{i+1} = C_1 l_{i+1} + C_2$ into $q_\pi(x_t, u_t) = \mathbb{E}_\pi \left[\sum_{i=t}^{\infty} \gamma^{i-t} r_{i+1} | x_t, u_t \right]$, then we obtain

$$\begin{aligned} q_\pi(x_t, u_t) &= \mathbb{E}_\pi \left[\sum_{i=t}^{\infty} \gamma^{i-t} (C_1 l_{i+1} + C_2) | x_t, u_t \right] \\ &= C_1 \mathbb{E}_\pi \left[\sum_{i=t}^{\infty} \gamma^{i-t} l_{i+1} | x_t, u_t \right] + C_2 \sum_{i=t}^{\infty} \gamma^{i-t} \\ &= C_1 \sum_{\forall x_{t+1} \in \mathbf{X}} \mathbf{P}_{x_t}^{x_{t+1}}(u_t) \mathbb{E}_\pi \left[\sum_{i=t+1}^{\infty} \gamma^{i-t} l_{i+1} | x_{t+1} \right] \\ &\quad + C_1 \mathbb{E} [l_{t+1} | x_t, u_t] + \frac{C_2}{1-\gamma} \\ &= C_1 \sum_{\forall x_{t+1} \in \mathbf{X}} \mathbf{P}_{x_t}^{x_{t+1}}(u_t) \lim_{N \rightarrow \infty} \mathbb{E}_\pi \left[\sum_{i=t+1}^N \gamma^{i-t} l_{i+1} | x_{t+1} \right] \\ &\quad + C_1 \mathbb{E} [l_{t+1} | x_t, u_t] + \frac{C_2}{1-\gamma} \\ &= C_1 \sum_{\forall x_{t+1} \in \mathbf{X}} \mathbf{P}_{x_t}^{x_{t+1}}(u_t) J_\pi(x_{t+1}) + C_1 \mathbb{E} [l_{t+1} | x_t, u_t] + \frac{C_2}{1-\gamma}. \end{aligned}$$

Recall that $\tilde{\pi}^*$ minimizes $J_\pi(x_{t+1}), \forall x_{t+1} \in \mathbf{X}$. Notice that only $C_1 \sum_{\forall x_{t+1} \in \mathbf{X}} \mathbf{P}_{x_t}^{x_{t+1}}(u_t) J_\pi(x_{t+1})$ depends on π in the last equality, where $C_1 < 0$. Hence, $\tilde{\pi}^*$ maximizes $q_\pi(x_t, u_t), \forall x_t \in \mathbf{X}, \forall u_t \in \mathbf{U}$. Now, it can be concluded that π^* is equivalent to $\tilde{\pi}^*$. ■

Theorem 1 shows how to design rewards such that the traditional optimal control problem can be solved in the framework of the Markov decision process, where π^* is equivalent to $\tilde{\pi}^*$. In the following, the algorithms for obtaining π^* , namely, *QL* and *DDQN*, are given.

C. Optimal Control of Small-scale PBCNs Using QL

For optimal infinite-horizon control of a small-scale PBCN, *QL* is used to obtain an optimal policy π^* . We define PBCNs as small-scale if and only if the memory of the action-values is within the RAM of the computer. Since a value takes 2^3 bytes, and 1 byte equals 2^{-10} GB, a PBCN is regarded as small-scale when 2^{m+n-7} is larger than the RAM (GB). For these problems, *QL* has two advantages. Firstly, *QL* is a model-free algorithm, which resolves the difficulty of modeling PBCNs. Secondly, *QL* has high computational efficiency, which ensures that an optimal control policy π^* can be obtained in a short time.

As shown in Figure 5, to facilitate the representation of action-values in a *Q*-table, states and actions are converted from binary to decimal. Before conversion, the vector forms of a state $x_t \in \mathcal{B}^n$ and an action $u_t \in \mathcal{B}^m$ are inconvenient for an action-value $Q(x_t, u_t)$ to be described in tabular form, so the conversion is considered. Convert x_t from binary to decimal:

$$x_t^D = \sum_{j=1}^n 2^{n-j} x_t(j), \quad (17)$$

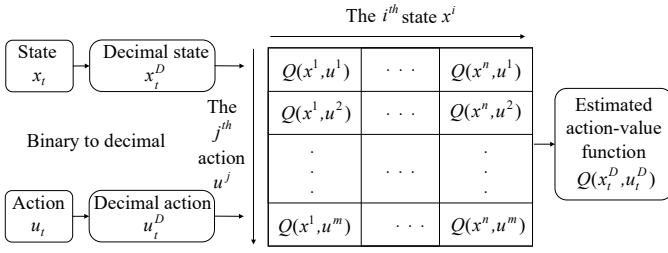


Fig. 5: Q -table for optimal infinite-horizon control of small-scale PBCNs

where $x_i(j)$, $j = 1, \dots, n$ is the j^{th} component of x_i . $x_i^D \in \mathbf{X}^D$ is the decimal state, where $\mathbf{X}^D = \{0, 1, \dots, 2^n - 1\}$. Similarly, convert u_i from binary to decimal:

$$u_i^D = \sum_{j=1}^m 2^{m-j} u_i(j), \quad (18)$$

where $u_i(j)$, $j = 1, \dots, m$ is the j^{th} component of u_i . $u_i^D \in \mathbf{U}^D$ is the decimal action, where $\mathbf{U}^D = \{0, 1, \dots, 2^m - 1\}$. After conversion, we can easily find $Q(x_i^D, u_i^D)$ in the u_i^{Dth} row and x_i^{Dth} column of the Q -table. In the following, Algorithm 1, namely, optimal infinity-horizon control of small-scale PBCNs using QL , is given.

Algorithm 1 Optimal infinite-horizon control of small-scale PBCNs using QL

Input:

Learning rate $\alpha_r \in (0, 1]$, discount factor $\gamma \in [0, 1)$, greedy rate $\epsilon \in [0, 1]$, maximum of episodes N , maximum of time steps T

Output:

Optimal control policy $\pi^*(x_i^D), \forall x_i^D \in \mathbf{X}^D$

- 1: Initialize $Q(x_i^D, u_i^D) \leftarrow 0, \forall x_i^D \in \mathbf{X}^D, \forall u_i^D \in \mathbf{U}^D$
- 2: **for** $ep = 0, 1, \dots, N - 1$ **do**
- 3: $x_0^D \leftarrow \text{rand}(\mathbf{X}^D)$
- 4: **for** $t = 0, 1, \dots, T - 1$ **do**
- 5: $u_t \leftarrow \begin{cases} \arg \max_{u_i^D \in \mathbf{U}^D} Q(x_t^D, u_i^D), & P = 1 - \epsilon \\ \text{rand}(\mathbf{U}^D), & P = \epsilon \end{cases}$
- 6: $Q(x_t^D, u_t^D) \leftarrow \alpha_r (r_{t+1} + \gamma \max_{u_i^D \in \mathbf{U}^D} Q(x_{t+1}^D, u_i^D)) + (1 - \alpha_r) Q(x_t^D, u_t^D)$
- 7: **end for**
- 8: **end for**
- 9: **return** $\pi^*(x_i^D) \leftarrow \arg \max_{u_i^D \in \mathbf{U}^D} Q(x_i^D, u_i^D), \forall x_i^D \in \mathbf{X}^D$

Algorithm 1 represents optimal infinite-horizon control of small-scale PBCNs using QL . An optimal deterministic control policy $\pi^*(x_i^D), \forall x_i^D \in \mathbf{X}^D$ is obtained through the algorithm. It is worth noting that the optimal deterministic control policy $\pi^*(x_i^D)$ is not necessarily unique, as an action-value $Q(x_i^D, u_i^D)$ may be maximized under multiple actions. Based on $\pi^*(x_i^D)$, the deterministic state feedback controller $u_t(x_i^D) = \pi^*(x_i^D)$ is obtained.

In Algorithm 1, ep means the number of episodes. ‘‘Episode’’ is a reinforcement learning term. An episode means

a period of interaction that has passed through T time steps from any initial state x_0^D . For optimal infinite-horizon control of PBCNs, the introduction of episode enriches an agent’s understanding of each state, so as to improve the control policy. Before introducing the episode, the agent interacts with the environment continuously from an initial state x_0^D . It is likely for the agent to experience only the adjacent states of x_0^D , but not other states. In this case, the control policy is limited.

The maximum of time steps T should be adjusted according to the scale of a PBCN and the difficulty of the control goal. Specifically, T increases with the difficulty of the control goal and the scale of a PBCN. If T is too small, the agent cannot obtain a positive reward before the end of an episode, so the learning speed will be affected. If T is too large, the agent will be in a situation similar to the no episode one, where the control policy is limited.

QL has a convergence guarantee, which ensures $\pi^*(x_i^D), \forall x_i^D \in \mathbf{X}^D$ obtained by Algorithm 1 approaches to the optimal one.

Theorem 2 [28]: $Q(x_i^D, u_i^D)$ converges to the fixed point $q^*(x_i^D, u_i^D)$ with probability one under the following conditions:

- 1) $\sum_{r=0}^{\infty} \alpha_r = \infty$ and $\sum_{r=0}^{\infty} \alpha_r^2 < \infty$, where $t' = ep \times T + t$ represents the global steps;
- 2) $\text{var}[r_t]$ is finite.

QL can effectively solve optimal infinite-horizon control of small-scale PBCNs, while $DDQN$ needs to be considered for large-scale ones. Specifically, the operation of QL is based on a Q -table with $|\mathbf{X}| \times |\mathbf{U}|$ values. For PBCNs, $|\mathbf{X}| \times |\mathbf{U}|$ increases exponentially with the number of nodes and control inputs. When the number of nodes in PBCNs is so large that $|\mathbf{X}| \times |\mathbf{U}|$ exceeds the computer memory, QL is no longer applicable. We define these PBCNs as large-scale. For large-scale PBCNs, consider $DDQN$. $DDQN$ uses function approximation that requires less memory than a Q -table to represent action-values, so it can effectively solve optimal infinite-horizon control of large-scale PBCNs.

D. Optimal Control of Large-scale PBCNs Using $DDQN$

In this section, π^* for optimal infinite-horizon control of large-scale PBCNs is obtained by $DDQN$. $DDQN$ has three advantages to the problem. Firstly, $DDQN$ is model-free, which solves the difficulty of modeling PBCNs. Secondly, $DDQN$ is suitable for problems with large state space, which makes it effective for large-scale PBCNs. Finally, $DDQN$ uses function approximation, which has strong generalization.

In the following, Algorithm 2 is given, which represents optimal infinite-horizon control of large-scale PBCNs using $DDQN$. An optimal deterministic control policy $\pi^*(x_i), \forall x_i \in \mathbf{X}$ is obtained through the algorithm. It is worth noting that π^* is not necessarily unique, as an action-value $Q(x_i, u_i, \theta)$ may be maximized under multiple actions. Based on $\pi^*(x_i)$, the deterministic state feedback controller $u_t(x_i) = \pi^*(x_i)$ is obtained.

The artificial neural network for optimal infinite-horizon control of PBCNs is shown in Figure 6. The inputs of the artificial neural network is the components of a state $x_i(i), i =$

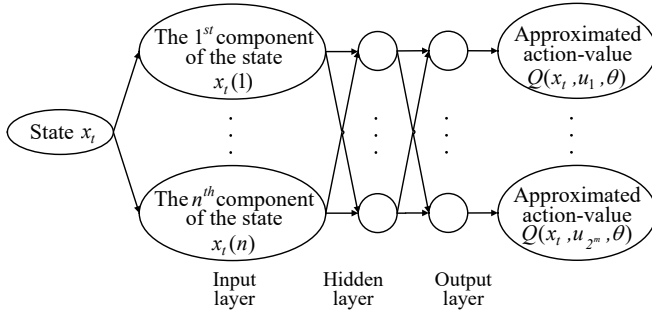


Fig. 6: Artificial neural network for optimal infinite-horizon control of large-scale PBCNs

$1, \dots, n$. This expression is a full and concise representation of the features of a state because reducing any one of the inputs will destroy the integrity, while increasing the inputs are not needed. Notice that the state x_t need not be to be converted from binary to decimal, since $[x_t(1), \dots, x_t(n)]$ is a natural one-hot vector which is a suitable input for the artificial neural network [37].

The setting of the replay memory capacity k and the mini-batch size M depends on the complexity of PBCN dynamics. Specifically, k and M rise with the number of nodes n , the number of control inputs m , and the number of available logic function $l_i, i \in 1, \dots, n$. If k or M is too small, samples stored in replay memory and used for network training cannot well represent PBCN dynamics, so the control policy is likely to be limited. If k or M is too large, the learning speed will be affected due to too much old-fashion experience.

Remark 2 : In this paper, we do not prove the convergence of Algorithm 2, which is based on DDQN. As two ANNs are used in calculating y_i , the behavior of DDQN becomes very complex. Thus, the convergence of DDQN is still an open problem, to the best of our knowledge.

E. Computational Complexity

DDQN is a combination of QL and deep learning. In terms of algorithm scalability, DDQN can solve large-scale problems that QL cannot. However, the time complexity of DDQN is significantly higher than that of QL.

Consider time complexity. In both QL and DDQN, an agent needs to select the control inputs with the optimal action-value from 2^m control inputs. The time complexity involved here is $O(2^m)$. In each episode of N episodes, this operation takes T steps. So, the total time complexity of this part is $O(NT2^m)$. In addition, it is necessary to update network parameters in DDQN, but not in QL. It is known that the number of nodes in the input layer and output layer is n and 2^m respectively. Assume that there is only 1 hidden layer with h nodes. Then, the time complexity involved in this part is $O(2^m h + hn)$. This operation also takes T steps in N episodes, where NT should rise with the growth of the state number 2^n and the complexity of the dynamics of the PBCNs [30]. So, the total time complexity of this part is $O(NT2^m h + NT hn)$. In a word, the additional operation of network updating makes the time complexity of DDQN higher than QL.

Algorithm 2 Optimal infinite-horizon control of large-scale PBCNs using DDQN

Input:

Learning rate $\beta \in (0, 1]$, discount factor $\gamma \in [0, 1]$, greedy rate $\epsilon \in [0, 1]$, maximum of episodes N , maximum of time steps T , mini-batch size M , target network learning rate $\tau \in [0, 1]$, replay memory capacity k

Output:

Optimal control policy $\pi^*(x_t), \forall x_t \in \mathbf{X}$

- 1: Initialize the main network parameter $\theta \leftarrow \text{rand}([0, 1])$
- 2: Initialize the target network parameter $\varphi \leftarrow \theta$
- 3: Initialize the replay memory $\mathcal{D}_k \leftarrow \emptyset$
- 4: **for** $ep = 0, 1, \dots, N - 1$ **do**
- 5: $x_0 \leftarrow \text{rand}(\mathbf{X})$
- 6: **for** $t = 0, 1, \dots, T - 1$ **do**
- 7: $u_t \leftarrow \begin{cases} \arg \max_{u_t \in \mathbf{U}} Q(x_t, u_t, \theta), & P = 1 - \epsilon \\ \text{rand}(\mathbf{U}), & P = \epsilon \end{cases}$
- 8: Take u_t , observe x_{t+1} and r_{t+1}
- 9: Store $(x_t, u_t, x_{t+1}, r_{t+1})$ at the rear of \mathcal{D}_k
- 10: **while** $|\mathcal{D}_k| \geq M$ **do**
- 11: Randomly select M sequences from \mathcal{D}_k
- 12: **for** $i = 0, 1, \dots, M - 1$ **do**
- 13: $y_i \leftarrow r_i + \gamma Q(x'_i, \arg \max_{u \in \mathbf{U}} Q(x'_i, u, \theta), \varphi)$
- 14: **end for**
- 15: $L(\theta) \leftarrow \frac{1}{M} \sum_{i=0}^{M-1} (y_i - Q(x_i, u_i, \theta))^2$
- 16: $\theta \leftarrow \theta - \alpha \nabla_{\theta} L(\theta)$
- 17: **end while**
- 18: $\varphi \leftarrow \beta \varphi + (1 - \beta) \theta$
- 19: **end for**
- 20: **end for**
- 21: **return** $\pi^*(x_t) = \arg \max_{u_t \in \mathbf{U}} Q(x_t, u_t, \theta), \forall x_t \in \mathbf{X}$

Consider space complexity. The space complexity of QL depends on the size of the Q -table. When the number of control inputs is m and the number of nodes is n , the space complexity involved in this part is $O(2^{n+m})$. The space complexity of DDQN depends on the size of network parameters θ and φ , and replay memory \mathcal{D}_k . It is known that the number of nodes in an input layer and an output layer is n and 2^m , respectively. Assume that there is only 1 hidden layer with h nodes. Then, the space complexity required by storing network parameters θ and φ is $O(2^{m+1} h + 2hn)$. To break the correlation between samples, the capacity of replay memory must be large enough. This increases the space complexity of DDQN significantly. Whether the space complexity of QL or DDQN is lower depends on the specific problem and parameter settings. Generally speaking, the space complexity of QL is lower for small-scale PBCNs, while the space complexity of DDQN is lower for large-scale PBCNs.

To sum up, QL is a better choice compared with DDQN in terms of time complexity. The advantage of DDQN is that it can solve optimal infinite-horizon control of large-scale PBCNs, while QL or model-based methods cannot. The next section uses an example to illustrate the applicability of DDQN in large-scale PBCNs. Specifically, DDQN is successfully

applied to optimal infinite-horizon control of the PBCN with 28 nodes and 3 control inputs, whose number of state-action pairs is 2.15×10^9 .

IV. SIMULATION

In this section, the performances of QL and $DDQN$ for optimal infinite-horizon control of PBCNs are analyzed and compared based on simulation. We consider two examples, which are a small-scale PBCN with 3 nodes and 1 control input, and a large-scale PBCN with 28 nodes and 3 control inputs. For each example, the change of the rewards in the training process and the obtained optimal controller are shown. For the small-scale PBCN, we analyze the optimal action-value errors and the optimal control policy errors in both QL and $DDQN$. From the errors, the convergence of QL and $DDQN$ is shown.

A. Examples

To evaluate the performance of the proposed algorithms, optimal action-value error $ErrorQ_{ep}$ and optimal control policy error $Error\pi_{ep}$ are defined. The optimal action-value error $ErrorQ_{ep}$ is the average absolute difference of optimal action-values between QL or $DDQN$ and policy iteration at the end of the episode ep :

$$ErrorQ_{ep} = \frac{1}{|\mathbf{X}|} \sum_{x \in \mathbf{X}} |v_{PI}^*(x) - \max_{u \in \mathbf{U}} Q_{ep}(x, u, \theta)|, \quad (19)$$

where $\max_{u \in \mathbf{U}} Q_{ep}(x, u, \theta)$ is the optimal action-value of the state x based on QL or $DDQN$ at the end of the episode ep , and $v_{PI}^*(x)$ is the optimal action-value of the state x obtained by policy iteration. Policy iteration is a model-based algorithm that converges to the optimal state-values and the optimal policy in finite-time [22]. Thus, it is reasonable to compare the optimal action-values and the optimal control policy obtained by QL or $DDQN$ with the ones obtained by policy iteration. Similarly, optimal control policy error $Error\pi_{ep}$ is the average absolute difference of the optimal control policy between QL or $DDQN$ and policy iteration at the end of the episode ep :

$$Error\pi_{ep} = \frac{1}{|\mathbf{X}|} \sum_{x \in \mathbf{X}} \|\pi_{PI}^*(x) - \pi_{ep}^*(x)\|, \quad (20)$$

where $\pi_{PI}^*(x)$ is the optimal action at the state x obtained by policy iteration, and $\pi_{ep}^*(x)$ is the one obtained by QL or $DDQN$ at the end of the episode ep . Notice that an optimal action of a PBCN is expressed as a vector $\pi^*(x) := (\pi_1^*(x), \dots, \pi_m^*(x)) \in \mathcal{B}^m$, which contains m elements. The distance between $\pi_{PI}^*(x)$ and $\pi_{ep}^*(x)$ under the norm $\|\cdot\|$ is the average difference between their components:

$$\|\pi_{PI}^*(x) - \pi_{ep}^*(x)\| = \frac{1}{m} \sum_{i=1}^m |\pi_{PI_i}^*(x) - \pi_{ep_i}^*(x)|, \quad (21)$$

where $\pi_{ep_i}^*(x)$ is the i^{th} component of $\pi_{ep}^*(x)$, and $\pi_{PI_i}^*(x)$ is the i^{th} component of $\pi_{PI}^*(x)$.

In the following examples, our control goals can be divided into two parts, which are to make control inputs and nodes

in the desired form. According to the two-part goal, l_{i+1} is expressed as follows:

$$l_{i+1}(x_t, u_t) = W_p P_{t+1} + W_h H_{t+1}. \quad (22)$$

In (22), $P_{t+1} = [p_{t+1}^1(u_t(1)), p_{t+1}^2(u_t(2)), \dots, p_{t+1}^m(u_t(m))]^T$ is the control input cost, where $p_{t+1}^i(u_t(i)) : \mathcal{B} \rightarrow \mathbb{R}^+$ is the cost of the i^{th} control input. $H_{t+1} = [h_{t+1}^1(x_t(1)), h_{t+1}^2(x_t(2)), \dots, h_{t+1}^n(x_t(n))]^T$ is the state cost, where $h_{t+1}^i(x_t(i)) : \mathcal{B} \rightarrow \mathbb{R}^+$ is the cost of the i^{th} node. $W_p = [w_{p1}, w_{p2}, \dots, w_{pm}]$ is the weight of the control input cost, where w_{pi} is the weight of $p_{t+1}^i(u_t(i))$. Besides, $W_h = [w_{h1}, w_{h2}, \dots, w_{hn}]$ is the weight of the state cost, where w_{hi} is the cost of $h_{t+1}^i(x_t(i))$. If one of our goals is to make $u_t(i), \forall t \in \mathbb{Z}^+$ in a specific form u_i^* , then $p_{t+1}^i(u_t(i))$ is defined as follows:

$$p_{t+1}^i(u_t(i)) = \begin{cases} 0, & \text{if } u_t(i) = u_i^*. \\ 1, & \text{else.} \end{cases} \quad (23)$$

Similarly, if another goal is to make $x_t(i), \forall t \in \mathbb{Z}^+$ in a specific form x_i^* , then $h_{t+1}^i(x_t(i))$ is defined as follows:

$$h_{t+1}^i(x_t(i)) = \begin{cases} 0, & \text{if } x_t(i) = x_i^*. \\ 1, & \text{else.} \end{cases} \quad (24)$$

If the i^{th} control input or the i^{th} node has no impact on the goal, then set $p_{t+1}^i(u_t(i)) = 0$ or $h_{t+1}^i(x_t(i)) = 0$. Besides, w_{pi} or w_{hi} depends on the importance of the i^{th} control input or the i^{th} node to the goal.

Example 1 : We consider the PBCN model of the apoptosis network given in [28]. The PBCN has 3 nodes $x_t = (x_t(1), x_t(2), x_t(3)) \in \mathcal{B}^3$ and 1 control input $u_t = (u_t(1)) \in \mathcal{B}^1$. The PBCN dynamics are given as follows:

$$\begin{cases} x_{t+1}(1) = f_1(x_t(1), x_t(2), x_t(3), u_t(1)), \\ x_{t+1}(2) = f_2(x_t(1), x_t(2), x_t(3), u_t(1)), \\ x_{t+1}(3) = f_3(x_t(1), x_t(2), x_t(3), u_t(1)), \end{cases} \quad t \in \mathbb{Z}^+, \quad (25)$$

where the logic functions are represented as follows:

$$\begin{cases} f_1^1(x_t(1), x_t(2), x_t(3), u_t(1)) = \neg x_t(2) \wedge u_t(1), & P_1^1 = 0.6, \\ f_1^2(x_t(1), x_t(2), x_t(3), u_t(1)) = u_t(1), & P_1^2 = 0.4, \\ f_2^1(x_t(1), x_t(2), x_t(3), u_t(1)) = \neg x_t(1) \wedge x_t(3), & P_2^1 = 0.7, \\ f_2^2(x_t(1), x_t(2), x_t(3), u_t(1)) = x_t(2), & P_2^2 = 0.3, \\ f_3^1(x_t(1), x_t(2), x_t(3), u_t(1)) = x_t(2) \vee u_t(1), & P_3^1 = 0.8, \\ f_3^2(x_t(1), x_t(2), x_t(3), u_t(1)) = x_t(3), & P_3^2 = 0.2. \end{cases} \quad (26)$$

Consider the optimal infinite-horizon control of the PBCN (25). We aim to find $\tilde{\pi}^*$ which minimizes the cost-to-go function:

$$J_{\tilde{\pi}}(x_t) = \lim_{N \rightarrow \infty} \mathbb{E}_{\tilde{\pi}} \left[\sum_{i=t}^N \gamma^{i-t} l_{i+1} | x_t \right], \quad \forall t \in \mathbb{Z}^+, \quad (27)$$

where the cost $l_{i+1}(x_t, u_t)$ is related to the control goals. One of the goals is to increase the activity of $x_t(2)$, i.e., let $x_t(2) = 1, \forall t \in \mathbb{Z}^+$ if possible. The goal is expressed as the state cost:

$$h_{t+1}^2(x_t(2)) = \begin{cases} 0, & \text{if } x_t(2) = 1. \\ 1, & \text{if } x_t(2) = 0. \end{cases} \quad (28)$$

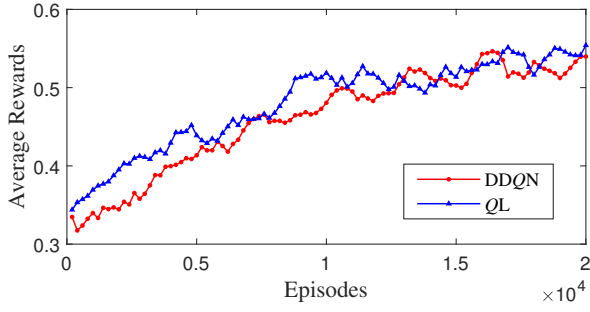


Fig. 7: Average rewards during training

Another goal is to make the control input $u_t(1) = 0, \forall t \in \mathbb{Z}^+$ if possible. This goal is expressed as the control input cost:

$$p_{t+1}^1(u_t(1)) = \begin{cases} 0, & \text{if } u_t(1) = 0. \\ 1, & \text{if } u_t(1) = 1. \end{cases} \quad (29)$$

Since $x_t(1)$ and $x_t(3)$ has nothing to do with the goal, set $h_{t+1}^1(x_t(1)) = 0$ and $h_{t+1}^3(x_t(3)) = 0$. Then, we define $w_{h2} = 0.8$ and $w_{p1} = 0.2$. According to (22), the cost is obtained as follows:

$$l_{t+1}(x_t, u_t) = \begin{cases} 0, & \text{if } u_t(1) = 0 \text{ and } x_t(2) = 1. \\ 0.2, & \text{if } u_t(1) = 1 \text{ and } x_t(2) = 1. \\ 0.8, & \text{if } u_t(1) = 0 \text{ and } x_t(2) = 0. \\ 1, & \text{if } u_t(1) = 1 \text{ and } x_t(2) = 0. \end{cases} \quad (30)$$

We turn the problem into finding π^* which maximizes the action-value function:

$$q_\pi(x_t, u_t) = \mathbb{E}_\pi \left[\sum_{i=t}^{\infty} \gamma^{i-t} r_{i+1} | x_t, u_t \right], \forall x_t \in \mathbf{X}, \quad (31)$$

where r_{i+1} is defined as $r_{i+1} = -l_{i+1} + 1$ to meet the condition of Theorem 1. The specific version of r_{i+1} is given as follows:

$$r_{i+1}(x_t, u_t) = \begin{cases} 1, & \text{if } u_t(1) = 0 \text{ and } x_t(2) = 1, \\ 0.8, & \text{if } u_t(1) = 1 \text{ and } x_t(2) = 1, \\ 0.2, & \text{if } u_t(1) = 0 \text{ and } x_t(2) = 0, \\ 0, & \text{if } u_t(1) = 1 \text{ and } x_t(2) = 0. \end{cases} \quad (32)$$

Following the above definition, we can conclude that π^* is equivalent to $\tilde{\pi}^*$. Then, Algorithms 1 and 2 are used to obtain π^* for optimal infinite-horizon control of the PBCN.

The average rewards in the training process by DDQN and QL are shown in Figure 7. The word ‘‘average’’ means taking an average of rewards in the neighboring 1000 episodes. The reason for taking the average is to reduce the influence of initial states on rewards, and then show the influence of training on rewards more objectively. The average rewards of both DDQN and QL keep rising from 0.35 to 0.55. For the training time, DDQN takes 2 hours, while QL only takes 10 seconds. From the above results and the time complexity, it can be concluded that QL is less time-consuming than DDQN in the optimal infinite-horizon control of PBCNs.

The convergence of DDQN and QL in the PBCN is shown in Figure 8. The variation of the optimal action-value errors $Error_{Q_{ep}}$ and the optimal control policy errors $Error_{\pi_{ep}}$ with

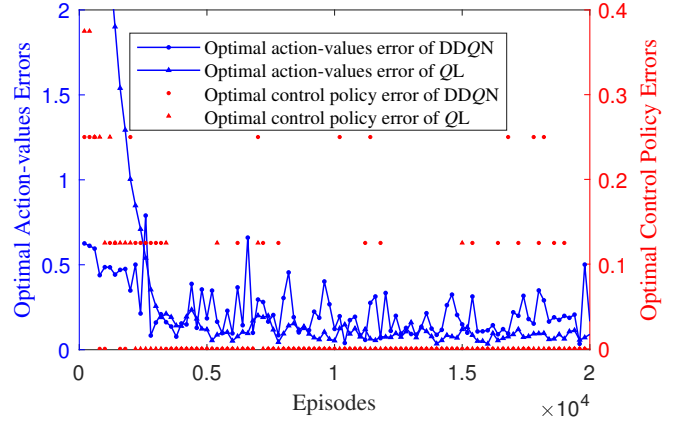


Fig. 8: Errors during training

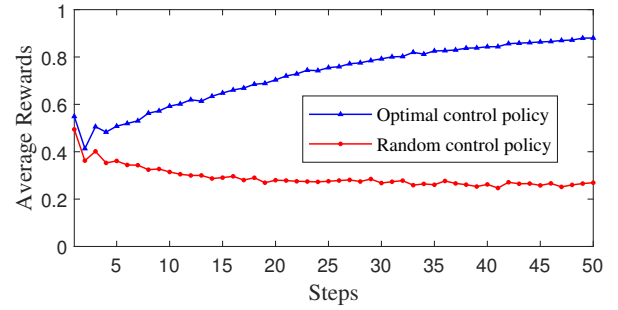


Fig. 9: Average rewards under optimal and random policy

the number of episodes are described. No matter DDQN or QL, the errors decrease with the increase of episode number. In the short run, the optimal control policy obtained from DDQN is more likely to approach the fixed point, while in the long run, the one obtained from QL is more likely to approach the fixed point. Therefore, for optimal infinite-horizon control of small-scale PBCNs, QL is more recommended if the number of training steps can be large enough. It is worth mentioning that at the end of the episode, the optimal control policy obtained from both DDQN and QL converges to the fixed point, which is:

$$\pi^*(x_t) = \begin{cases} 1, & \text{if } x_t = (0, 0, 0) \text{ or } x_t = (1, 0, 0). \\ 0, & \text{others.} \end{cases} \quad (33)$$

Remark 3: The policy (33) obtained by DDQN and QL is exactly the same as the one according to policy iteration [21]–[25], which shows the optimality of (33).

The effect of optimal controller obtained is shown in Figures 9 and 10. Figure 9 describes the average rewards according to the optimal control policy, and presents the ones according to the random control policy as a comparison. The word ‘‘average’’ means taking an average of rewards in 1000 repeated experiments with random initial states. The reason for taking an average is to reduce the influence of initial states on rewards, so as to describe the effect of optimal control policy on rewards more objectively. As shown in Figure 9, the average rewards according to the optimal control policy are significantly greater than that according to the random control

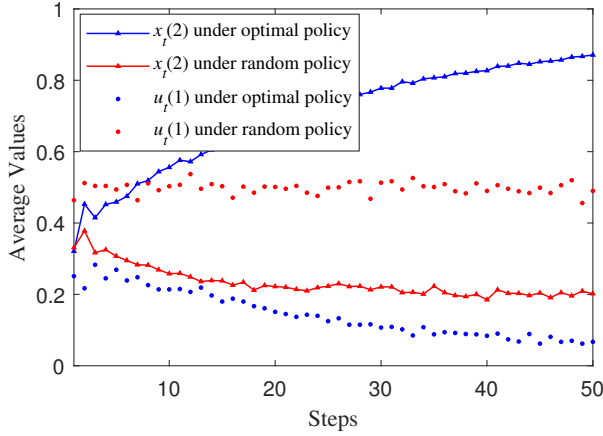


Fig. 10: Average values under optimal and random policy

policy. In particular, according to the optimal control policy, the average rewards increase from 0.4 to 0.9 with the number of steps, which are close to the maximum reward 1. In contrast, according to the random control policy, the average rewards fluctuate around 0.3, far from the maximum reward 1. Figure 10 describes the average value of the target gene activity $x_t(2)$ and the target control input $u_t(1)$ according to the optimal control policy, and the ones according to the random policy control as a comparison. Similarly, the word “average” means taking an average of rewards in 1000 repeated experiments with random initial states. As shown in Figure 10, the average values of $x_t(2)$ and $u_t(1)$ according to the optimal control policy are closer to the control goal than that according to the random control policy. To be specific, according to the optimal control policy, $x_t(2)$ increases from 0.3 to 0.9 with the number of steps, which is close to the control goal 1, and $u_t(1)$ decreases from 0.2 to 0.05, which is close to the control goal 0. In contrast, according to the random control policy, $x_t(2)$ decreases from 0.3 to 0.2, while $u_t(1)$ fluctuates around 0.5, far from the control goal.

Remark 4 : In our paper, the system model is presented only for illustrating the problem, but the agent has no knowledge of it.

Example 2 : We consider the PBCN model of the reduced-order T-cell given in [32]. The PBCN has 28 nodes $x_t = (x_t(1), \dots, x_t(28)) \in \mathcal{B}^{28}$ and 3 control inputs $u_t = (u_t(1), u_t(2), u_t(3)) \in \mathcal{B}^3$. The PBCN dynamics are abbreviated as follows:

$$\begin{aligned}
 &x_1^+ = x_6 \wedge x_{13}; \quad x_2^+ = x_{25}; \quad x_3^+ = x_2; \quad x_4^+ = x_{28}; \quad x_5^+ = x_{21}; \quad x_6^+ = x_5; \\
 &x_7^+ = (x_{15} \wedge u_2) \vee (x_{26} \wedge u_2); \quad x_8^+ = x_{14}; \quad x_9^+ = x_{18}; \quad x_{10}^+ = x_{25} \wedge x_{28}; \\
 &x_{11}^+ = \neg x_9; \quad x_{12}^+ = x_{24}; \quad x_{13}^+ = x_{12}; \quad x_{14}^+ = x_{28}; \quad x_{15}^+ = (\neg x_{20})u_1 \wedge u_2; \\
 &x_{16}^+ = x_3; \quad x_{17}^+ = \neg x_{11}; \quad x_{18}^+ = x_2; \quad x_{19}^+ = (x_{10} \wedge x_{11} \wedge x_{25} \wedge x_{28}) \vee (x_{11} \wedge x_{23} \wedge x_{25} \wedge x_{28}); \\
 &x_{20}^+ = x_7 \vee \neg x_{26}; \quad x_{21}^+ = x_{11} \vee x_{22}; \quad x_{22}^+ = x_2 \wedge x_{18}; \quad x_{23}^+ = x_{15}; \quad x_{24}^+ = x_{18}; \quad x_{25}^+ = x_8; \\
 &x_{26}^+ = \neg x_4 \wedge u_3, \quad \mathbf{P} = 0.5 \quad x_{26} = x_{26}, \quad \mathbf{P} = 0.5; \quad x_{27}^+ = x_7 \vee (x_{15} \wedge x_{26}); \\
 &x_{28}^+ = \neg x_4 \wedge x_{15} \wedge x_{24},
 \end{aligned} \tag{34}$$

where x_i represents the activity of the i^{th} gene at the current

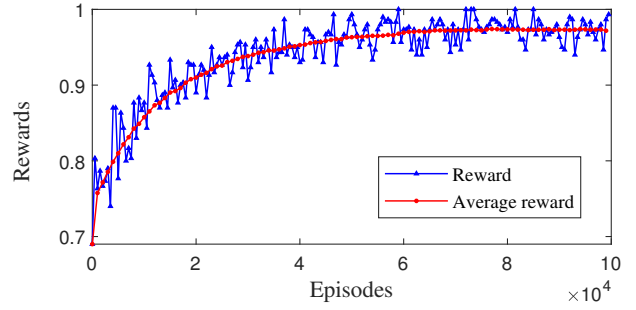


Fig. 11: Rewards during training

time step, and x_i^+ represents the activity of the i^{th} gene at the next time step.

We consider the optimal infinite-horizon control of the PBCN (34). We aim to find $\tilde{\pi}^*$ which minimizes the cost-to-go function in (16):

$$J_{\tilde{\pi}}(x_t) = \lim_{N \rightarrow \infty} \mathbb{E}_{\tilde{\pi}} \left[\sum_{i=t}^N \gamma^{i-t} l_{i+1} | x_t \right], \forall t \in \mathbb{Z}^+, \tag{35}$$

where $l_{i+1}(x_t, u_t)$ is related to the control goal. One of the control goals is to decrease the activity of $x_t(1)$ and $x_t(7)$, i.e., let $x_t(1) = 0$ and $x_t(7) = 0$. The goal is expressed as the state cost, which is given as follows:

$$h_{i+1}^i(x_t(i)) = \begin{cases} 0, & \text{if } x_t(i) = 0, \\ 1, & \text{if } x_t(i) = 1, \end{cases} \quad i \in \{1, 7\}. \tag{36}$$

Another goal is to make control inputs be the ones $u_t(1) = 0$, $u_t(2) = 0$, and $u_t(3) = 0$ if possible. The goal is expressed as the control input cost, which is given as follows:

$$p_{i+1}^i(u_t(i)) = \begin{cases} 0, & \text{if } u_t(i) = 0, \\ 1, & \text{if } u_t(i) = 1, \end{cases} \quad i \in \{1, 2, 3\}. \tag{37}$$

In addition to the mentioned nodes, others do not affect the goal. So, $h_{i+1}^i(x_t(i)) = 0$, $i \neq 1$ and $i \neq 7$. Then, we define $w_{h1} = 0.4$, $w_{h7} = 0.3$, $w_{p1} = 0.1$, $w_{p2} = 0.1$, and $w_{p3} = 0.1$. The cost is obtained according to (22).

We define $r_{i+1} = -l_{i+1} + 1, \forall i \in \mathbb{Z}^+$. Then, according to Theorem 1, the problem is turned into finding π^* which maximizes the action-value function:

$$q_{\pi}(x_t, u_t) = \mathbb{E}_{\pi} \left[\sum_{i=t}^{\infty} \gamma^{i-t} r_{i+1} | x_t, u_t \right], \forall x_t \in \mathbf{X}. \tag{38}$$

The PBCN (34) has 28 nodes and 3 control inputs. The corresponding number of the action-values is 2.15×10^9 , which is so large that QL or model-based methods like policy iteration are no longer applicable. For optimal infinite-horizon control of large-scale PBCNs, DDQN is used to obtain optimal control policies.

The rewards and the average rewards in the training process of DDQN are described in Figure 11. The word “average” means taking an average of rewards in the neighboring 1000 episodes. As the number of episodes increases, both the rewards and the average rewards keep rising, close to the maximum reward 1. The average rewards increase fast in the first 60000 episodes, and almost stop rising and converge in

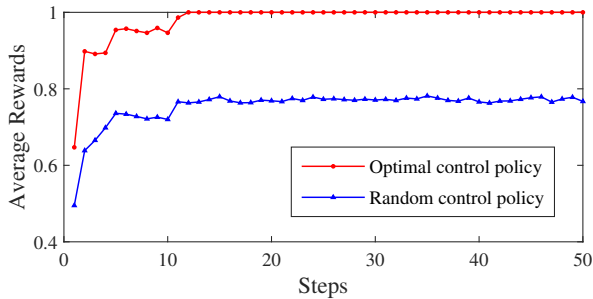


Fig. 12: Average rewards under optimal and random policy

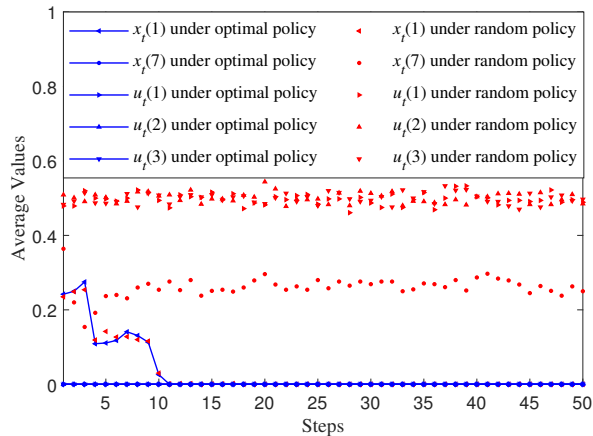


Fig. 13: Average values under optimal and random policy

the later 40000 episodes. The growth trend of the rewards is basically consistent with the one of the average rewards. Taking the average rewards as the reference, the rewards float with ± 1 as the episodes change, which is mainly due to the difference in initial states. As the scale of a PBCN increases, the maximum number of episodes and time steps also increase, which leads to a longer training time, i.e., 56 hours.

The effect of the optimal controller obtained by DDQN is shown in Figures 12 and 13. Figure 12 describes the average rewards according to the optimal control policy, and presents the ones according to the random control policy as a comparison. The word ‘‘average’’ means taking an average of rewards in 1000 repeated experiments with random initial states. As shown in Figure 12, the average rewards according to the optimal control policy are significantly greater than that according to the random control policy. In particular, according to the optimal control policy, the average rewards increase from 0.9 to the maximum reward 1 with the number of steps. In contrast, according to the random control policy, the average rewards increase from 0.65 to 0.8, far from the maximum reward 1. Figure 13 describes the average value of the target gene activity $x_t(1)$ and $x_t(7)$ and the control inputs $u_t(1)$, $u_t(2)$, and $u_t(3)$ according to the optimal policy control, and the ones according to the random policy control as a comparison. As shown in Figure 13, the average values of $x_t(1)$, $x_t(7)$, $u_t(1)$, $u_t(2)$, and $u_t(3)$ according to the optimal control policy are close to the control goal. To be specific, according to the optimal control policy, $x_t(1)$, $x_t(7)$, $u_t(1)$, $u_t(2)$, and $u_t(3)$ all

TABLE I: Parameter settings

Example	N	T	\mathcal{M}	k	h	δ
1	2×10^4	15	128	5×10^4	2	8×10^{-6}
2	1×10^5	30	256	2×10^5	16	2×10^{-6}

decrease to the control goal 0 at the time step 11. In contrast, according to the random control policy, $x_t(7)$ fluctuates around 0.25, and all the control inputs fluctuate around 0.5, far from the control goal.

From the above results, it is concluded that DDQN can solve the infinite-horizon optimal control of large-scale PBCNs, thus having certain advantages over the methods in previous literatures. Model-based optimal control mostly uses semi-tensor product and policy iteration [21]–[25]. These methods are based on matrix operation, so they are not suitable for large-scale PBCNs, generally speaking, the ones with more than 20 nodes. In contrast, we propose DDQN, which can handle large-scale PBCNs. Besides, the sample-based method using path integral given by [16] has two advantages, which are model-free and applicable to large-scale PBCNs. However, the method can only give the optimal policy according to a given initial state. Compared with [16], the optimal policy can be obtained without knowledge of initial states in our method, due to the strong generalization of DDQN.

B. Pattern and Details

The simulation was completed on a 6-Core Intel i5-6200U processor with a frequency of 2.30GHz, and 12GB RAM. The software which we used is MATLAB R2021a. QL and policy iteration were implemented by scripts, and DDQN was implemented by the Reinforcement Learning Designer Toolbox.

In terms of parameter selection, for both Examples 1 and 2, we chose the same discount factor $\gamma = 0.9$, target network learning rate $\beta = 0.001$, the number of hidden layers $n_h = 1$, and rectified linear units (ReLU) as activation function. In Example 1, we set the learning rate for QL as a generalized harmonic series $a_r = 1/(ep + 1)^\omega$ where $\omega = 0.6$, which satisfies conditions 1) and 2) in Theorem 2. According to the complexity of Examples 1 and 2, we selected different maximum number of episodes N , maximum number of time step T , mini-batch size \mathcal{M} , replay memory capacity k , the number of nodes in a hidden layer h , and decay rate of greedy rate δ . The specific parameter settings are shown in Table I. Besides, we defined greedy rate as $\epsilon = (1 - \delta)^t$.

V. CONCLUSION

In this paper, a deep reinforcement learning based method is proposed to obtain optimal infinite-horizon control policies for PBCNs. In particular, we establish the connection between action-value functions in deep reinforcement learning and cost-to-go functions in traditional optimal control. Then, QL and DDQN are applied to optimal infinite-horizon control of small-scale PBCNs and large-scale PBCNs, respectively. Meanwhile,

the optimal state feedback controllers are designed. The proposed method in this paper has two advantages. First, both QL and $DDQN$ are model-free techniques, which resolve the difficulty of modeling PBCNs. Second, $DDQN$ can solve optimal infinite-horizon control of large-scale PBCNs while many algorithms cannot. Through the discussion of computational complexity and the simulation, we compare the advantages of QL and $DDQN$. The advantage of QL over $DDQN$ lies in its convergence guarantee and small time complexity. Therefore, optimal control policies can be obtained through QL with higher accuracy in a shorter time. However, the premise of QL is that the memory required for action-values is within the RAM of the computer. Therefore, we defined the small-scale PBCNs to which QL is applicable as those that meet the memory requirement. And for others, we recommend using $DDQN$, which can solve problems with large state space. It is worth mentioning that although the convergence of $DDQN$ has not been proved theoretically, its convergence can be found experimentally in our simulation.

REFERENCES

- [1] S. Kauffman, "Metabolic stability and epigenesis in randomly constructed genetic nets," *Journal of Theoretical Biology*, vol. 22, no. 3, pp. 437–467, 1969.
- [2] I. Shmulevich, E. R. Dougherty, S. Kim, and W. Zhang, "Probabilistic Boolean networks: a rule-based uncertainty model for gene regulatory networks," *Bioinformatics*, vol. 18, no. 2, pp. 261–274, 2002.
- [3] F. Li and J. Sun, "Controllability of probabilistic Boolean control networks," *Automatica*, vol. 47, no. 12, pp. 2765–2771, 2011.
- [4] M. Toyoda and Y. Wu, "On optimal time-varying feedback controllability for probabilistic Boolean control networks," *IEEE Transactions on Neural Networks and Learning Systems*, vol. 31, no. 6, pp. 2202–2208, 2020.
- [5] C. Huang, J. Lu, D. W. Ho, G. Zhai, and J. Cao, "Stabilization of probabilistic Boolean networks via pinning control strategy," *Information Sciences*, vol. 510, pp. 205–217, 2020.
- [6] F. Li and L. Xie, "Set stabilization of probabilistic Boolean networks using pinning control," *IEEE Transactions on Neural Networks and Learning Systems*, vol. 30, no. 8, pp. 2555–2561, 2019.
- [7] R. Li, M. Yang, and T. Chu, "State feedback stabilization for probabilistic Boolean networks," *Automatica*, vol. 50, no. 4, pp. 1272–1278, 2014.
- [8] H. Li, X. Yang, and S. Wang, "Perturbation analysis for finite-time stability and stabilization of probabilistic Boolean networks," *IEEE Transactions on Cybernetics*, vol. 51, no. 9, pp. 4623–4633, 2021.
- [9] Y. Liu and H. Li, "Logical matrix factorization towards topological structure and stability of probabilistic Boolean networks," *Systems & Control Letters*, vol. 149, p. 104878, 2021.
- [10] Y. Guo, R. Zhou, Y. Wu, W. Gui, and C. Yang, "Stability and set stability in distribution of probabilistic Boolean networks," *IEEE Transactions on Automatic Control*, vol. 64, no. 2, pp. 736–742, 2019.
- [11] E. Fornasini and M. E. Valcher, "Observability and reconstructibility of probabilistic Boolean networks," *IEEE Control Systems Letters*, vol. 4, no. 2, pp. 319–324, 2020.
- [12] R. Zhou, Y. Guo, and W. Gui, "Set reachability and observability of probabilistic Boolean networks," *Automatica*, vol. 106, pp. 230–241, 2019.
- [13] A. Yerudkar, C. D. Vecchio, and L. Glielmo, "Output tracking control of probabilistic Boolean control networks," in *2019 IEEE International Conference on Systems, Man and Cybernetics (SMC)*, 2019, pp. 2109–2114.
- [14] A. Zhang, L. Li, Y. Li, and J. Lu, "Finite-time output tracking of probabilistic Boolean control networks," *Applied Mathematics and Computation*, vol. 411, p. 126413, 2021.
- [15] B. Faryabi, A. Datta, and E. Dougherty, "On approximate stochastic control in genetic regulatory networks," *IET Systems Biology*, vol. 1, pp. 361–368(7), 2007.
- [16] S. Kharade, S. Sutavani, S. Wagh, A. Yerudkar, C. Del Vecchio, and N. Singh, "Optimal control of probabilistic Boolean control networks: A scalable infinite horizon approach," *International Journal of Robust and Nonlinear Control*, pp. 1–22, 2021.
- [17] Y. Wu and T. Shen, "Policy iteration approach to control residual gas fraction in ic engines under the framework of stochastic logical dynamics," *IEEE Transactions on Control Systems Technology*, vol. 25, no. 3, pp. 1100–1107, 2017.
- [18] T. Z. Q. Liu, X. Guo, "Optimal control for probabilistic Boolean networks," *IET Systems Biology*, vol. 4, pp. 99–107(8), 2010.
- [19] Y. Wu and T. Shen, "An algebraic expression of finite horizon optimal control algorithm for stochastic logical dynamical systems," *Systems & Control Letters*, vol. 82, pp. 108–114, 2015.
- [20] Q. Zhu, Y. Liu, J. Lu, and J. Cao, "On the optimal control of Boolean control networks," *SIAM Journal on Control and Optimization*, vol. 56, no. 2, pp. 1321–1341, 2018.
- [21] R. Pal, A. Datta, and E. Dougherty, "Optimal infinite-horizon control for probabilistic Boolean networks," *IEEE Transactions on Signal Processing*, vol. 54, no. 6, pp. 2375–2387, 2006.
- [22] Y. Wu and T. Shen, "Policy iteration algorithm for optimal control of stochastic logical dynamical systems," *IEEE Transactions on Neural Networks and Learning Systems*, vol. 29, no. 5, pp. 2031–2036, 2018.
- [23] Y. Wu, X.-M. Sun, X. Zhao, and T. Shen, "Optimal control of Boolean control networks with average cost: A policy iteration approach," *Automatica*, vol. 100, pp. 378–387, 2019.
- [24] Y. Wu, Y. Guo, and M. Toyoda, "Policy iteration approach to the infinite horizon average optimal control of probabilistic Boolean networks," *IEEE Transactions on Neural Networks and Learning Systems*, vol. 32, no. 7, pp. 2910–2924, 2021.
- [25] E. Fornasini and M. E. Valcher, "Optimal control of Boolean control networks," *IEEE Transactions on Automatic Control*, vol. 59, no. 5, pp. 1258–1270, 2014.
- [26] D. Bertsekas, *Reinforcement learning and optimal control*. Athena Scientific, 2019.
- [27] Watkins, P. Christopher JCH, and Dayan, "Q-learning," *Machine Learning*, vol. 8, no. 3, pp. 279–292, 1992.
- [28] T. Jaakkola, M. Jordan, and S. Singh, "Convergence of stochastic iterative dynamic programming algorithms," in *Advances in Neural Information Processing Systems*, vol. 6. Morgan-Kaufmann, 1993.
- [29] R. S. Sutton and A. G. Barto, *Reinforcement learning: An introduction*. MIT press, 2018.
- [30] A. Acernese, A. Yerudkar, L. Glielmo, and C. D. Vecchio, "Reinforcement learning approach to feedback stabilization problem of probabilistic Boolean control networks," *IEEE Control Systems Letters*, vol. 5, no. 1, pp. 337–342, 2021.
- [31] P. Bajaria, A. Yerudkar, and C. D. Vecchio, "Random forest Q-Learning for feedback stabilization of probabilistic Boolean control networks," in *2021 IEEE International Conference on Systems, Man, and Cybernetics (SMC)*, 2021, pp. 1539–1544.
- [32] M. Volodymyr, K. Koray, S. David, A. A. Rusu, V. Joel, M. G. Bellemare, G. Alex, R. Martin, A. K. Fijeland, and O. a. Georg, "Human-level control through deep reinforcement learning," *Nature*, vol. 518, no. 7540, pp. 529–533, 2015.
- [33] H. V. Hasselt, A. Guez, and D. Silver, "Deep reinforcement learning with double Q-learning," *Proceedings of the AAAI Conference on Artificial Intelligence*, pp. 1–13, 2016.
- [34] G. Papagiannis and S. Moschogiannis, "Deep reinforcement learning for control of probabilistic Boolean networks," in *Complex Networks & Their Applications IX*. Springer International Publishing, 2021, pp. 361–371.
- [35] A. Acernese, A. Yerudkar, L. Glielmo, and C. D. Vecchio, "Double deep-q learning-based output tracking of probabilistic Boolean control networks," *IEEE Access*, vol. 8, pp. 199 254–199 265, 2020.
- [36] T. Tao, *An introduction to measure theory*. Providence: American Mathematical Society, 2011.
- [37] A. Géron, *Hands-on machine learning with Scikit-Learn, Keras, and TensorFlow*. O'Reilly Media, Inc., 2022.